Effect of an interchain magnetic interaction on the dimerized state of a two-XY-quantum-spin-chain ladder

Laurent Hubert and Alain Caillé
Centre de Recherche en Physique du Solide et Département de Physique, Université de Sherbrooke, Sherbrooke, Québec, Canada, J1K 2R1
(Received 2 July 1990; revised manuscript received 26 December 1990)

The model that we study is a two-XY-quantum-spin-chain system with Ising interchain magnetic interaction. This model, referred to as the spin-ladder model, is used as a first step to model the thermodynamic properties of low-dimensional spin system. Similarities between the spin-ladder model and the one-dimensional Hubbard model are used in our analysis. As a consequence we can qualitatively understand the heat capacity and spin susceptibilty and show that both measurements are necessary to analyze a spin-ladder system. We also show that the strong-interchain-coupling limit of the spin-ladder model is equivalent to a one-chain spin Heisenberg Hamiltonian. Furthermore, the spin-Peierls transition is investigated for small ($|I/2J| \ll 1$) and large ($|I/2J| \gg 1$) interchain coupling, and we show its occurrence at relatively small spin-phonon coupling ($\lambda \lesssim 0.6$). From the results obtained for the small- and large-interchain-interaction limits, we propose the conjecture that the in-phase dimerization persists for all values of the interaction parameter at zero temperature.

I. INTRODUCTION

Materials—mainly organic compounds—which are good candidates to show the spin-Peierls transition have been available for two decades.[1-3] In spite of their apparent overall similarity, some of these compounds show the spin-Peierls transition characteristics, whereas others do not. To understand the difference in behavior, previous works studied effects due to external magnetic field,[4-7] and distant-neighbor[9,10] elastic terms, anisotropy in the magnetic coupling,[10-13] magnetostriction,[11,12] etc., of an independent (sole) magnetic chain. We consider, as a further step in this spin-Peierls study, the introduction of an interchain magnetic interaction I. We show that, depending on their relative size, the magnetic interchain interaction can compete against or enhance the nonlocal intrachain magnetic interaction J and phonon interaction.

Our interest in the interchain magnetic coupling is also justified by the existence of real spin-ladder systems as will be shown below. In the absence of a proper theoretical treatment of the spin ladder, the interpretation of the experimental results of such a system is confined to two extreme choices. One is to compare the magnetic susceptibility for spin-ladder-like compounds with numerical data derived for the Heisenberg dimerized spin chain and then associate the magnetic gap of the former with the dimerization gap of the later.[14] The other choice is to consider the spin ladder, even at low temperature, as composed of two independent spin chains.[15,16] In this paper we show how the observed behavior can be derived from a spin-ladder model and show the necessity of heat-capacity measurements to verify or to improve the interpretation of the susceptibility data.

The treatment of quantum spin-chain coupling is a difficult task by itself. In fact, the numerical work of Dagotto and Moreo,[17] for the ground-state energy and gap of an Heisenberg spin ladder with $I/J=1$, is one of the very few[16] attempts in that direction. To make progress we decided to treat the simplest interacting model that we could envisage, i.e., the two spin-half XY chains with an Ising interchain magnetic interaction as in Fig. 1. This model, which can be seen as a crude approximation for the more general problem of many spin chains in magnetic interaction, is used to give preliminary results and insights into the general case. Otherwise, it can be applicable to actual systems of two-[14-16,18,19] or three[20]-spin-chain materials that can have effective Ising, XY spin coupling (see, for example, Ref. 21) or a mix of both, coming from spin-orbit coupling coupled with crystal-field anisotropy. Far from being completely artificial, this model may be viewed as combining both the XY and Ising interactions, which are the archetype, respectively, of all easy-plane and all easy-axis magnetizations. Using a Jordan-Wigner-type transformation, the spin-ladder model is mapped on a pseudofermion version of the generalized Hubbard model.[22] A detailed study of the similarities and differences of the two models allows us to use the known results of the Hubbard model to predict the behavior of the spin-ladder problem.

The paper is divided as follows. In Sec. II we present the Hamiltonian of the spin-ladder model, its order-parameter operators and its symmetries in terms of spin-half operators and of pseudofermion operators. Thermodynamic properties are presented and discussed in Sec. III for some special cases of the nondimerized spin ladder. In Sec. IV, we introduce elastic degrees of freedom in the system. The study of the effect of small (Sec. IV A) and large (Sec. IV B) magnetic interchain couplings on the dimerization capability of the system is carried

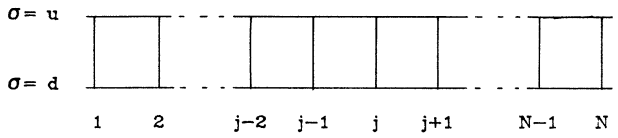

FIG. 1. Schematic representation of a ladderlike two spin-half chains with Heisenberg or XY intrachain spin coupling and Ising interchain interaction. j is the rung index number and σ the chain index.

through comparing the energies of two different dimerization states (in phase and antiphase) and the uniform state. Conclusions and final discussions end the paper in Sec. V.

II. THE SPIN-LADDER MODEL AND ITS PROPERTIES

The physical properties of the model introduced above are determined by the following Hamiltonian:

$$H=\sum_{\sigma}\sum_{j}J_{j,\sigma}(S^{x}_{j,\sigma}S^{x}_{j+1,\sigma}+S^{y}_{j,\sigma}S^{y}_{j+1,\sigma}) -g\mu_{B}\sum_{\sigma}\sum_{j}h_{\sigma,j}S^{z}_{j,\sigma} +\sum_{\sigma}\sum_{j}J_{j,\sigma}\gamma S^{z}_{j,\sigma}S^{z}_{j+1,\sigma}+I\sum_{j}S^{z}_{j,u}S^{z}_{j,d}\ , \tag{2.1}$$

$j=1,2,\ldots,N$ is the rung index and $\sigma=u,d$ (up, down) is the chain index. The $J_{j,\sigma}$ and I are, respectively, the intrachain and Ising interchain first neighbor magnetic exchange interactions. A term of interaction with an external field $h_{j,\sigma}$ in the z direction is included where g and μ_B have their usual meaning. The anisotropy of the intrachain exchange is given by $(1-\gamma)$. For future use, we define the following operators:

$$\mathcal{O}_{P}(q)=\sum_{\sigma}\sum_{j}e^{iqaj}S^{z}_{j,\sigma}\ , \tag{2.2a}$$

$$\mathcal{O}_{A}(q)=\sum_{\sigma}\sum_{j}e^{iqaj}\delta_{\sigma}S^{z}_{j,\sigma}\ , \tag{2.2b}$$

$$\mathcal{O}_{\mathrm{STW}}(q,\sigma)=\sum_{j}e^{iqaj}(S^{+}_{j,\sigma}S^{-}_{j+1,\sigma}+\mathrm{H.c.})\ , \tag{2.2c}$$

$$\theta(\sigma)=\tfrac{1}{2}\mathcal{O}_{\mathrm{STW}}(\pi/a,\sigma)+\gamma\sum_{j}e^{i\pi j}S^{z}_{j,\sigma}S^{z}_{j+1,\sigma}\ , \tag{2.2d}$$

where $S^{\pm}_{j,\sigma}=S^{x}_{j,\sigma}\pm iS^{y}_{j,\sigma}$, a is the intrachain lattice parameter, $\delta_u=1$, $\delta_d=-1$, and H.c. means the Hermitian conjugate of the previous term. The order parameters associated with the operators $\mathcal{O}_P$ and $\mathcal{O}_A$ correspond, respectively, to two spin-density waves of wave number q (SDW) (one on each chain) mutually in phase (P) or in antiphase (A). On the other hand, $\mathcal{O}_{\mathrm{STW}}(\sigma)$ is associated with a spin-transfer wave (STW) order parameter of wave number q on the chain σ. Finally, $\theta(\sigma)$, the operator associated with the total transfer fluctuations at $q=\pi/a$, drives the chain σ toward dimerization.

For $h_\sigma=0$, $I=0$, $\gamma=1$ in (2.1), the total spin operator of the chain σ and the total spin operator of the spin ladder, respectively, $S_\sigma=\sum_j S_{j,\sigma}$ and $S=S_u+S_d$ produce good quantum numbers. But, for the general case, only S^{z}_{σ} and S^{z} commute with the Hamiltonian (2.1). In order to illustrate other transformation properties of this Hamiltonian, let us consider the unitary transformation T which consists of a 180° rotation in the y-z plane of all the spins belonging to the chain $\sigma=d$;

$$\tilde{\mathbf{S}}_{j,\sigma}=T^{-1}\mathbf{S}_{j,\sigma}T\ ,$$

where

$$T=\exp\left[i\pi\sum_{j}S^{x}_{j,d}\right]\ . \tag{2.3}$$

Operators with a tilde are the transformed operators. Under T, the Hamiltonian (2.1) and the two order-parameter operators $\mathcal{O}_P$ and $\mathcal{O}_A$ transform as

$$\begin{aligned}T^{-1}H(J_{j\sigma},I,h_u,h_d)T&=\tilde{H}(J_{j\sigma},I,h_u,h_d)\\&=H(J_{j\sigma},-I,h_u,-h_d)\ ,\\T^{-1}\mathcal{O}_{P}(q)T&=\tilde{\mathcal{O}}_{P}(q)=\mathcal{O}_{A}(q)\ ,\\T^{-1}\mathcal{O}_{A}(q)T&=\tilde{\mathcal{O}}_{A}(q)=\mathcal{O}_{P}(q)\ .\end{aligned} \tag{2.4}$$

The two other operators $\mathcal{O}_{\mathrm{STW}}(\sigma)$ and $\theta(\sigma)$ are invariant under the transformation T. An interesting result, for $h_{j,\sigma}=0$, follows directly. In that special case, the two Hamiltonians $H(I)$ and $H(-I)$ are the same operator expressed in two different bases linked by an unitary transformation. They have identical eigenvalue spectra. Thus for $h_{j,\sigma}=0$, thermodynamic properties such as the free energy, the total energy, and the heat capacity are even functions of I. This statement is valid for any modulation of the exchange integral $J_{j,\sigma}$, including the case of dimerization where it is easy to show that the dimerization gap and amplitude are even functions of I.

The Hamiltonian (2.1) and the order-parameter operators (2.2) may be written in terms of pseudofermion (PF) operators using a unitary (but noncanonical) transformation. The following Jordan-Wigner transformations are used:

$$\begin{aligned}a_{j,d}&=S^{-}_{j,d}\prod_{\nu=1}^{j-1}(-2S^{z}_{\nu,d})\ ,\\a_{j,u}&=S^{-}_{j,u}\prod_{\mu=1}^{N}(-2S^{z}_{\mu,d})\prod_{\nu=1}^{j-1}(-2S^{z}_{\nu,u})\ ,\end{aligned} \tag{2.5}$$

where $\hbar=1$. The $a_{j,u\,(d)}$ and their Hermitian conjugates obey the fermion anticommutation relations. Notice that the index σ acts as a spin-$\frac{1}{2}$ quantum number of the PF. Using (2.5), Eqs. (2.2) become

$$\begin{aligned}\mathcal{O}_{P}(q)&\rightarrow\mathcal{O}^{f}_{\mathrm{CDW}}(q)=\sum_{\sigma j}e^{iqaj}n_{j,\sigma}\ ,\\\mathcal{O}_{A}(q)&\rightarrow\mathcal{O}^{f}_{\mathrm{SDW}}(q)=\sum_{\sigma j}e^{iqaj}\delta_{\sigma}n_{j\sigma}\ ,\\\mathcal{O}_{\mathrm{STW}}(q,\sigma)&\rightarrow\mathcal{O}^{f}_{\mathrm{CTW}}(q,\sigma)\\&=\sum_{j}e^{iqaj}(a^{\dagger}_{j,\sigma}a_{j+1,\sigma}+\mathrm{H.c.})\ ,\\\theta(\sigma)&\rightarrow\tfrac{1}{2}\mathcal{O}^{f}_{\mathrm{CTW}}(\pi/a,\sigma)+\gamma\sum_{j}e^{i\pi j}n_{j,\sigma}n_{j+1,\sigma}\\&\quad-\frac{\gamma}{2}\mathcal{O}^{f}_{\mathrm{CDW}}(\pi/a,\sigma)\ .\end{aligned} \tag{2.6}$$

In the fermion representation, indicated by the superscript f; $\mathcal{O}^f_{\rm CDW}$ is a charge-density wave operator, $\mathcal{O}^f_{\rm SDW}$ a spin-density wave operator, and $\mathcal{O}^f_{\rm CTW}(\sigma)$ a charge-transfer wave operator for the pseudofermions of index σ. Note, at this point, the similarity of the order parameter operators of the ladder system when expressed in pseudofermions with those of the one-dimensional conductor problem. The Hamiltonian (2.1) in term of pseudofermions becomes

$$H=H_0+H_\gamma+H_c+C \ , \tag{2.7}$$

where

$$H_0=\tfrac{1}{2}\sum_{\sigma j}J_{j,\sigma}(a^\dagger_{j,\sigma}a_{j+1,\sigma}+\text{H.c.}) \ ,$$

$$H_I=\sum_{\sigma j}\left[J_{j,\sigma}\gamma n_{j,\sigma}n_{j+1,\sigma}+\frac{I}{2}n_{j,\sigma}n_{j,-\sigma}\right] \ ,$$

$$H_c=-\sum_{\sigma j}\left[\frac{I}{2}+g\mu_B h_\sigma+\frac{\gamma}{2}(J_{j,\sigma}+J_{j-1,\sigma})\right]n_{j,\sigma} \ ,$$

and

$$C=+\frac{N}{2}g\mu_B(h_u+h_d)+\frac{NI}{4}+\frac{\gamma}{4}\sum_{\sigma j}J_{j,\sigma} \ .$$

Here $-\sigma$ is the opposite value of σ (i.e., if $\sigma=u$ then $-\sigma=d$). This Hamiltonian is a special case of the extended Hubbard model. Notice the absence of interaction terms between first-neighbor pseudofermions of opposite index. An important aspect of this pseudofermion description of the spin-ladder problem is that the number of pseudofermions is subject to fluctuations contrary to the electronic situation where their number is an external constraint.

In order to establish the correspondence between the different response functions of the ladder spin system and the extended Hubbard model, the unitary transformation (2.3) is applied to the pseudofermion operators to give

$$\begin{aligned}&T^{-1}a_{j,d}T=\tilde{a}_{j,d}=-a^\dagger_{j,d}e^{i\pi j} \ , \\ &T^{-1}a_{j,u}T=\tilde{a}_{j,u}=a_{j,u}(-1)^N \ ,\end{aligned} \tag{2.8}$$

with corresponding expressions for their Hermitian conjugates. From (2.2) we observe that the magnetic susceptibility response $\bar{\chi}_{L,+}(q,I)$ $[\bar{\chi}_{L,-}(q,I)]$ for the spin ladder to a magnetic field $h_u=h_d$ $(h_u=-h_d)$ is the response function of the order parameter associated with $\mathcal{O}_P(q)$ $[\mathcal{O}_A(q)]$. On the other hand, the "magnetic susceptibility" of the spin-$\frac{1}{2}$ pseudofermions, $\bar{\chi}_{QF}(q,I)$, is the response of the order parameter associated with $\frac{1}{2}\mathcal{O}^f_{\rm SDW}(q)$ or $\frac{1}{2}\mathcal{O}_A(q)$.

These generalized susceptibilities are defined by

$$\begin{aligned}&\bar{\chi}_{L,+}(q,I,\omega)=\int_{-\infty}^{\infty}dt\,e^{i\omega t}\langle\,\mathcal{T}[\mathcal{O}^\dagger_P(q,I,t)\mathcal{O}_P(q,I)]\rangle \ , \\ &\bar{\chi}_{L,-}(q,I,\omega)=\int_{-\infty}^{\infty}dt\,e^{i\omega t}\langle\,\mathcal{T}[\mathcal{O}^\dagger_A(q,I,t)\mathcal{O}_A(q,I)]\rangle \ , \\ &\bar{\chi}_{\rm PF}(q,I,\omega)=\tfrac{1}{4}\int_{-\infty}^{\infty}dt\,e^{i\omega t}\langle\,\mathcal{T}[\mathcal{O}^\dagger_A(q,I,t)\mathcal{O}_A(q,I)]\rangle \ .\end{aligned} \tag{2.9}$$

$\mathcal{T}$ is the time-ordering operator, ω is the frequency, and $\langle\cdots\rangle$ is the thermodynamic average. Defining the susceptibility per spin and the susceptibility per pseudofermion, respectively, by $\chi_{L,\pm}(q,I,\omega)=(1/2N)\bar{\chi}_{L,\pm}(q,I,\omega)$ and $\chi_{\rm PF}(q,I,\omega)=(1/N)\bar{\chi}_{\rm PF}(q,I,\omega)$, the properties of transformation illustrated in (2.4) lead to the important result

$$\chi_{L,\pm}(q,I,\omega)=2\chi_{\rm PF}(q,\mp I,\omega) \ . \tag{2.10}$$

Thus, the magnetic susceptibility obtained for the pseudofermion model can be used to evaluate the susceptibility of the spin ladder system.

III. THE *XY*-ISING LADDER AND ITS PROPERTIES

With $\gamma=0$ (XY intrachain) and $h_\sigma=0$, the Hamiltonian (2.7) becomes

$$\begin{aligned}H=&1/2\sum_{\sigma,j}J_{j,\sigma}(a^\dagger_{j,\sigma}a_{j+1,\sigma}+\text{H.c.})+I\sum_j n_{j,u}n_{j,b} \\ &-(I/2)\sum_{\sigma,j}(n_{j,\sigma}-\tfrac{1}{2}) \ .\end{aligned} \tag{3.1}$$

This Hamiltonian is identical to the grand canonical half-filled one-band Hubbard Hamiltonian,[22] with the chemical potential μ equal to $I/2$. Under this condition, (3.1) has quasiparticle-quasihole symmetry. This symmetry is a necessary but not a sufficient condition to infer that the band of PF is half-filled. However this conclusion is reached using an explicit calculation of the total energy as a function of band filling $n=1/N\sum_{\sigma j}\langle n_{j,\sigma}\rangle$ for some value of interchain interaction I. This calculation is done using the Lieb and Wu[23] solution of the following Hamiltonian:

$$H_U=\sum_{\sigma,j}t(a^\dagger_{j,\sigma}a_{j+1,\sigma}+\text{H.c.})+I\sum_j n_{j,\uparrow}n_{j,\downarrow} \ , \tag{3.2}$$

where $\sigma=\uparrow$ or $\downarrow$, $n_{j,\sigma}=a^\dagger_{j,\sigma}a_{j,\sigma}$, and $a^\dagger_{j,\sigma}$ $(a_{j,\sigma})$ is a creation (annihilation) operator for an electron of spin σ at site j. For an arbitrary filling level the solution of (3.2) is given by coupled integral equations. We approximate it by a set of 41 algebraic equations (see Ref. 24 for a similar calculation). Using our unit of energy $(J_{j,\sigma}/2=J/2=t)$ and adding the contribution of the third term of (3.1) $(NI/2)(1/2-n)$, it is easily verified that for all value of I considered (Fig. 2) the energy of the fundamental of the spin ladder, $E_f(n,I)$, is minimal for a half-filled band $(n=1)$. Thus the average z component of the spins in the two-spin chain ladder is zero $(\langle S^z\rangle=0)$. The fundamental of (3.2) is known from Lieb and Wu to be a singlet. For the spin ladder, this means that the wave function of the fundamental is antisymmetric with respect to the exchange of chains, and that $\langle S^z_u\rangle=\langle S^z_b\rangle$. Therefore, we conclude that for the uniform spin ladder (i.e., $J_{j,\sigma}=J$), $\langle S^z_u\rangle=\langle S^z_b\rangle=\langle S^z\rangle=0$ in the fundamental. The energy of our system is written as

$$E_f=-2NJ\int_0^\infty\frac{J_0(x)J_1(x)}{x(\exp(x|I|/J)+1)}dx-\frac{|I|N}{4} \ , \tag{3.3a}$$

where J_0 and J_1 are Bessel functions of the first kind, re-

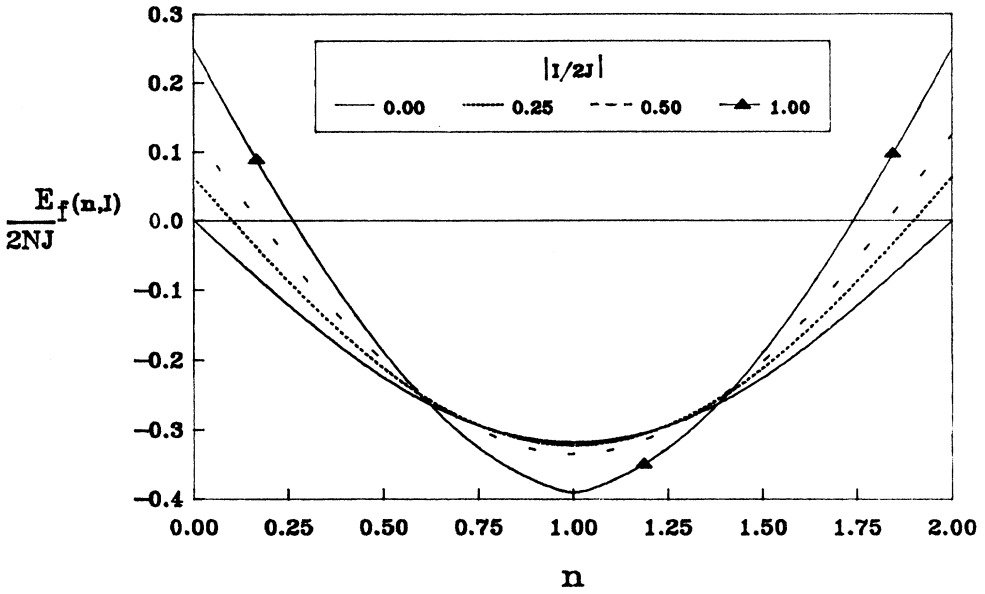

FIG. 2. Energy per spin of the XY-Ising spin ladder with respect to the occupation level n for different values of interchain coupling, $|I/2J|=0.00, 0.25, 0.50, 1.00$. The minimum appears for the half-filled band case ($n=1$).

spectively, of order zero and one. This result is obtained by adding $(NI/2)(1/2-n)=-NI/4$ to the Lieb-Wu solution and by putting $|I|$ instead of I to ensure that $E_f(-I)=E_f(I)$ as was established in Sec. II [see discussion following Eq. (2.3)]. For $I=0$ we recover (see Fig. 3) the energy by site for isolated XY chains, $-J/\pi$. For $|I/2J|\gg 1$, the limit of independent rungs, $E_f(I)\approx -N|I|/4$ (dotted curve) is achieved.

Using a theorem due to Feynman,[25] average intrarung and interrrung spin-correlation functions (P_c and K_c) are calculated with

$$\partial E_f/\partial I=\sum_j \langle S^z_{j,u}S^z_{j,d}\rangle_f$$
$$=NP_c$$
$$=-\frac{IN}{2|I|}\int_0^\infty J_0(x)J_1(x)\tanh^2\left[\frac{x|I|}{2J}\right]dx \tag{3.3b}$$

and

$$\partial E_f/\partial J=\sum_{j,\sigma}\langle S^x_{j,\sigma}S^x_{j+1,\sigma}+S^y_{j,\sigma}S^y_{j+1,\sigma}\rangle_f$$
$$=2NK_c$$
$$=\frac{1}{J}E_f-\frac{I}{J}\frac{\partial}{\partial I}E_f\ , \tag{3.3c}$$

where $\langle\cdots\rangle_f$ means that only the fundamental state is considered. We put $\partial|I|/\partial I=|I|/I$. At the independent-chain limit, $I=0$, $P_c=0$, and $K_c=1/\pi$. For large value of $|I/2J|$, P_c saturates to $\pm|I|/4$ and K_c goes to zero. This shows that in the strongly interacting case, there are only parallel spins ($I<0$) or antiparallel spins ($I>0$) on each rung and the spin exchange along a chain is frozen out as the interchain interaction increases (Fig. 3 for graphical result).

Along with the Hubbard model,[26,27] the spin-ladder system has gap and gapless excitations. For $I>0$ ($I<0$), the gapless excitations regroup, at first order of perturbation, configurations that have antiparallel (parallel) spins on each rung, the corresponding order operators being $\mathcal{O}_A(q)$ [$\mathcal{O}_P(q)$] and their energy spectrum is linear in q for small q. The gap excitations regroup those configurations that have parallel (antiparallel) spins at least on one rung, their operators being $\mathcal{O}_P(q)$ [$\mathcal{O}_A(q)$] and the gap in the energy spectrum is $\Delta_L\approx|I|/2$ for

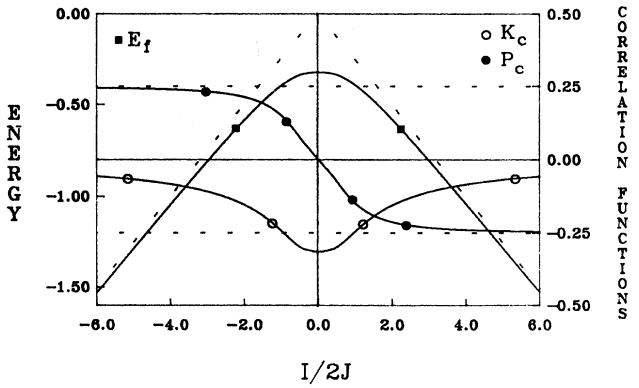

FIG. 3. The XY-Ising spin ladder energy E_f, the interchain correlation function P_c, and the intrachain correlation function K_c as functions of the interchain coupling $I/2J$. All quantities are evaluated in the fundamental of the uniform state.

large $|I|$. The lowest energy state above the gap are those that have $\langle S^z\rangle=\pm 1$ ($n=1\pm 1/N$). These excited states have no equivalent in the Hubbard model ($\mu=I/2$, $\Delta_U\approx I$) where n is fixed by external constraint. As shown in Sec. IV B, the large coupling limit of the spin ladder is equivalent to the Heisenberg antiferromagnetic Hamiltonian ($1d$) with exchange constant $J^2/2|I|$.

These general characteristics of the energy spectrum along with the Hubbard model results[28–30] lead to a simple qualitative understanding of the temperature dependence of the heat capacity by spin $C_v(T)$ of the XY-Ising ladder model. The main features in the strong coupling limit (large $|I/2J|$) are the presence of two maxima identified by T_1 and T_2 in Fig. 4 and produced, respectively, by gap and gapless excitations. In the $J\to 0$ limit, with the absence of the gapless excitations, the main feature of the specific heat $C_v(T)$ of the spin ladder is simply the Schottky anomaly for two sharp levels separated by an energy $I/2$:

$$C_v(J\to 0,T)=\tfrac{1}{2}k_B(\beta I/4)^2\mathrm{sech}^2(\beta I/4)\ ,$$

where $\beta=1/k_BT$. The maximum [$C_v(T_1)\cong 0.22k_B$] appears at $k_BT_1=0.83|I|/4$. The same expression is obtained for the heat capacity of the half-filled one-band Hubbard model with zero bandwidth ($t\to 0$). The effect of $J\neq 0$; which delocalizes the gap excitations, reduces their minimum energy and increases quantum fluctuation effects, is to enlarge the specific heat peak at T_1 with accompanying reduction of both its height and its central position (T_1). At low temperature, the gapless excitations give rise to the linear behavior of $C_v(T)$ for $T\ll T_2$ where $k_BT_2\approx J^2/2|I|$. For $T_2<T<T_1$, there is a gradual decrease $\approx(k_BT)^{-2}$ until contributions from the gap excitations appear and the Heisenberg chain equivalence is lost. For small coupling, $|I/2J|\ll 1$, both maxima overlap and merge toward the position of the maximum of the independent XY chain ($I=0$): $k_BT\approx 0.65J/2$.

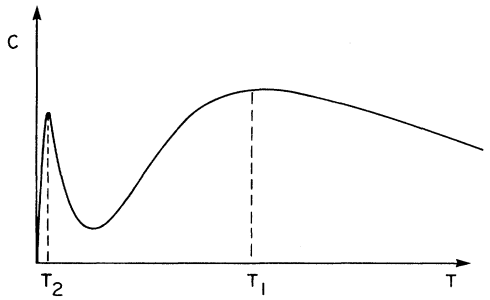

FIG. 4. Specific heat of the spin ladder in arbitrary unit for high interchain coupling $|I/2J|\gg 1$. The behavior is independent of the sign of the interaction I, only the source of this behavior as a sign dependency. For $I>0$ ($I<0$) the low temperature peak, T_2, comes from gapless excitations of antiparallel (parallel) pairs of spin and the high temperature peak, T_1, comes from gap excitation from "broken" pairs.

Let us look at the general features of the magnetic susceptibility per spin. We limit ourselves to in-phase and antiphase responses of the two magnetic chains. Consider the following mean-field Hamiltonian, H_{MF};

$$H_{\mathrm{MF}}=\sum_{\sigma,j}\frac{J}{2}(S^x_{j,\sigma}S^x_{j+1,\sigma}+S^y_{j,\sigma}S^y_{j+1,\sigma})-g\mu_B\sum_{\sigma,j}h_\sigma\cos(qja)S^z_{j,\sigma}+I\sum_j(S^z_{j,u}\langle S^z_{j,d}\rangle+\langle S^z_{j,u}\rangle S^z_{j,d}-\langle S^z_{j,u}\rangle\langle S^z_{j,d}\rangle)\ ,$$

where random $\langle S^z_{j,\sigma}\rangle$ is determined self-consistently. The random-phase approximation (RPA) susceptibility is given by

$$\langle S^z_{j,\sigma}\rangle=\sum_i\chi_{\mathrm{RPA},\pm}(j-i)h_{i,\sigma}$$
$$=\sum_i\chi_0(j-i)[(g\mu_B)^2h_{i,\sigma}-I\langle S^z_{i,-\sigma}\rangle] \qquad (3.4)$$

and after taking the Fourier transform, (3.4) becomes

$$\chi_{\mathrm{RPA},\pm}(q,T)=(g\mu_B)^2\frac{\chi_0(q,T)}{1\pm I\chi_0(q,T)}\ , \qquad (3.5)$$

where

$$(g\mu_B)^2\chi_0(q,T)=2(g\mu_B)^2\sum_k\frac{f(\varepsilon_k)-f(\varepsilon_{k+q})}{\varepsilon_{k+q}-\varepsilon_k}$$

is the susceptibility of the independent chains, $f(\varepsilon_k)$ is the Fermi distribution function, and $\varepsilon_k=-|J|\cos(ka)$. Finally the $+$ ($-$) in $\pm$ is obtained if $h_u=h_d$ ($h_u=-h_d$). Note that for $I<0$ ($I>0$), $\chi_{\mathrm{RPA},+}(q,T)$ increases (decreases) from the $I=0$ situation and that $\chi_{\mathrm{RPA},-}(q,T)$ has the opposite behavior. Stoner's criterion[31] indicates, from (3.5), a "phase transition" when $1\pm I\chi_0(q,T)=0$. Even though the singular behavior is an artifact of the use of a mean field theory for the low dimensional system, it signals the onset of increasing short-range correlations of a particular type. Since $\chi_0(q,T)$ has a finite value, it is needed to have $\pm I>1/\max[\chi_0(q,T)]$ to be related to a highly correlated thermodynamic state. Finally, it should be noted that $\chi_{\mathrm{RPA},-}(q,T)$ is identical to the RPA susceptibility of the Hubbard model.[32,33] This should however correctly describe the high temperature dependence, especially for small $|I/2J|$, and for the dependence on the sign of I. Other informations, for the large interchain coupling limit of a uniform spin ladder are obtainable from the equivalent Heisenberg model treated in Sec. IV. In that case, the low temperature dependence of $\chi_-(q,I>0)$ and $\chi_+(q,I<0)$ of our spin-ladder model are equivalent to the magnetic susceptibility of a Heisenberg chain. In

fact, numerical data[29] show that this equivalence persists, at least qualitatively, over a wide range of temperature and of $|I/2J|$ ratio. As a result we have an alternative way to obtain low temperature Heisenberg spin chain magnetic behavior for a spin-ladder structure.[14–16] On the other hand $\chi_-(q,I<0)$ and $\chi_+(q,I>0)$ are reduced by an order of magnitude mainly because all the excitations involved are above the gap. Starting from zero at $T=0$,[34] they increase exponentially with temperature until $k_\beta T \approx I$ and then decrease very slowly at higher temperature.

This section shows clearly that great care should be used in the interpretation of the susceptibility data of a spin ladder. It shows also that heat capacity can be a better tool to probe strong interchain interaction. In that context, this measurement, made with the susceptibility, can improve greatly the analysis of a spin ladder.

IV. THE DIMERIZED STATES AT $T=0$ K

In this section the effect of interchain interaction on the dimerization amplitude and gap of the XY-Ising ladder is studied. We consider two types of dimerization and show which is preferred over the other. The elastic energy is introduced by adding an intrachain free phonon part to Hamiltonian (3.1):

$$H_p=\frac{K}{2}\sum_{\sigma,j}(u_{j+1,\sigma}-u_{j,\sigma})^2 , \tag{4.1}$$

where $\sigma=u$, d and $u_{j,\sigma}$ is the longitudinal displacement of site (j,σ) from its position in the uniform state. The intrachain spin-phonon interaction is written using the first-order expansion of $J_{j,\sigma}$ with respect to longitudinal displacement:

$$J_{j,\sigma}=J+J'_{j,\sigma}(u_{j+1,\sigma}-u_{j,\sigma}) , \tag{4.2}$$

where $J'_{j,\sigma}$ is the derivative of $J_{j,\sigma}$ with respect to the length of the jth bond. From quantization of the phonon field, bosons operators $b_{j,\sigma}$, with a two-value σ index, is introduced. Here, the spin-boson interaction comes only when both have the same σ index. A perturbative expansion of the spin-phonon interaction shows that this interaction is like a retarded interaction between spins of same index σ. Mean-field spin-phonon interaction gives

$$J_{j,\sigma}=J[1-(-1)^j\delta_\sigma] , \tag{4.3}$$

where $\delta_\sigma=(J'/J)\langle u_{j,\sigma}-u_{j+1,\sigma}\rangle(-1)^j$ is the dimerization parameter. The σ index on δ_σ permits us to introduce a difference in the elastic modulation of the two chains.

We consider the "in phase" (P) dimerization, $\delta_u=\delta_d=\delta$, and the "antiphase" (A) dimerization, $\delta_u=-\delta_d=\delta$. Using (2.6), the associated order operators for these two dimerizations are written as

$$\begin{aligned}\mathcal{O}_{TP}&=\mathcal{O}^f_{\mathrm{CTW}}(q=\pi/a,\sigma=u)\\&\quad+\mathcal{O}^f_{\mathrm{CTW}}(q=\pi/a,\sigma=d) ,\\ \mathcal{O}_{TA}&=\mathcal{O}^f_{\mathrm{CTW}}(q=\pi/a,\sigma=u)\\&\quad-\mathcal{O}^f_{\mathrm{CTW}}(q=\pi/a,\sigma=d) ,\end{aligned} \tag{4.4}$$

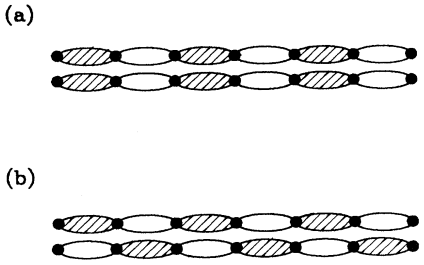

FIG. 5. Schematic representation of the order parameter associated with (a) $\mathcal{O}^f_{TP}$ and (b) $\mathcal{O}^f_{TA}$. The dots are the spin positions. Regions of spin transfer densities are described by bubbles. Dark and light bubbles are, respectively, for high and small transfer densities.

where T means transfer of pseudofermions and $\mathcal{O}^f_{\mathrm{CTW}}(q,\sigma)$ is related to $\mathcal{O}_{\mathrm{STW}}(q,\sigma)$ of Eq. (2.2c) by Jordan-Wigner transformation. Schematic representations of $\mathcal{O}_{TP}$ and $\mathcal{O}_{TA}$ are given in Fig. 5. Note that if one wants to talk about the dimerization of the Heisenberg-Ising ladder, one needs to replace, in (4.4), $\mathcal{O}^f_{\mathrm{CTW}}(q=\pi/a,\sigma)$ by the pseudofermion representation of $\theta(\sigma)$ [Eq. (2.2d)]. The problem, in this last case, is similar to the introduction of a modulation of the intersite electron-electron interaction in the extended Hubbard model. Staying with the XY-Ising ladder, the following response functions for each kind of dimerization are written

$$\begin{aligned}N_{TP}(q,\omega)&=\int_{-\infty}^{\infty}dt\,e^{i\omega t}\langle\mathcal{T}(\mathcal{O}^\dagger_{TP}(t)\mathcal{O}_{TP}(0))\rangle ,\\ N_{TA}(q,\omega)&=\int_{-\infty}^{\infty}dt\,e^{i\omega t}\langle\mathcal{T}(\mathcal{O}^\dagger_{TA}(t)\mathcal{O}_{TA}(0))\rangle .\end{aligned} \tag{4.5}$$

From (4.5) and (4.4) we see that cross terms $\mathcal{O}^f_{\mathrm{CTW}}(q=\pi/a,\sigma,t)\mathcal{O}^f_{\mathrm{CTW}}(q=\pi/a,-\sigma,(0))$ and $\mathcal{O}^f_{\mathrm{CTW}}(q=\pi/a,-\sigma,t)\mathcal{O}^f_{\mathrm{CTW}}(q=\pi/a,\sigma,(0))$ are multiplied by -1 in N_{TA} and by $+1$ in N_{TP}. Then, it is clear that N_{TP} and N_{TA} can have behaviors very different when correlations between chains occur. This, with more details, is studied in the following subsections.

A. Small interchain coupling case

Before using a variational method, more has to be said about the fluctuations of $\langle S^z\rangle$. In the case of independent chains these fluctuations are produced by occupation fluctuations at the Fermi level and the energy variation of the system is of the order of $\Delta\varepsilon_{kf}\sim J/N$. A gap, $J\Gamma\gg\Delta\varepsilon_{kf}$, at the Fermi level, as it happens with dimerization, reduces extensively these fluctuations and the system is pinned on a $\langle S^z\rangle=0$ state. We make the working hypothesis that a small interchain interaction will not strongly reduce this effect. As a result we take $\langle S^z\rangle=0$ and $n=1$ and we will not consider fluctuations of these quantities. Based on these assumptions we utilize the Gutzwiller's ansatz as used by Baeriswyl and Maki.[35] The Hamiltonian H for XY-Ising ladder with mean-field spin-phonon interaction is rewritten as

$$H=\tfrac{1}{2}J\mathcal{J}+I\mathcal{V}\ , \tag{4.6}$$

where

$$\mathcal{J}=\sum_{\sigma,j}[1-(-1)^j\delta_\sigma](a^\dagger_{j,\sigma}a_{j+1,\sigma}+\text{H.c.})$$

and

$$\mathcal{V}=NP_c=\sum_j n_{j,u}n_{j,d}-N/4\ ,$$

where P_c is given by (3.3b). A particular state $|\Psi\rangle$, defined by

$$|\Psi\rangle=\exp(-\eta W/2)|0\rangle\ , \tag{4.7}$$

is written, where $|0\rangle$ is the fundamental state of the mean-field Hamiltonian H_d:

$$H_d=\frac{J}{2}\sum_{\sigma,j}[1-(-1)^j\Gamma_\sigma](a^\dagger_{j,\sigma}a_{j+1,\sigma}+\text{H.c.})\ , \tag{4.8}$$

η is a pseudoparticle-pseudoparticle correlation parameter and W is given by

$$W=\sum_j n_{j,u}n_{j,d}\ . \tag{4.9}$$

$J\Gamma_\sigma$ is a mean-field energy gap produced by the dimerization. This gap is not necessarily proportional to δ_σ as it happens for XY independent chains. The variational method is applied on the functional energy $\varepsilon(\eta,\delta_h,\delta_b,\Gamma_h,\Gamma_b)$ per site:

$$\varepsilon=\frac{J}{8\pi\lambda}\sum_\sigma\delta_\sigma^2+\frac{\langle\Psi|H|\Psi\rangle}{2N\langle\Psi|\Psi\rangle}\ , \tag{4.10}$$

where $\lambda=J'^2/2\pi JK$ is the spin-phonon coupling constant. Note that instead of (4.9) we can use

$$W=\sum_j(n_{j,u}-\tfrac{1}{2})(n_{j,d}-\tfrac{1}{2})=\mathcal{V}\ . \tag{4.11}$$

It does not change (4.10) because $\sum_{\sigma,j}n_{j,\sigma}$ commutes with H and H_d.

From P_c (Fig. 3) we know that the configuration that has antiparallel (parallel) spins on each rung has, for positive (negative) I, larger weight in $|\Psi\rangle$ than those with parallel (antiparallel) spins on some rungs. Then from (4.7) and (4.11) it is expected that η has the same sign as I. Applying the transformation (2.8) on (4.6), (4.7), (4.8), and (4.11) one verifies that

$$\frac{\langle\Psi(\eta)|H(I)|\Psi(\eta)\rangle}{\langle\Psi(\eta)|\Psi(\eta)\rangle}=\frac{\langle\Psi(-\eta)|H(-I)|\Psi(-\eta)\rangle}{\langle\Psi(-\eta)|\Psi(-\eta)\rangle}\ . \tag{4.12}$$

Expansion of the exponential of (4.11) in powers of η shows that only connected diagrams contribute to the energy:

$$\begin{aligned}\frac{\langle\Psi|H|\Psi\rangle}{\langle\Psi|\Psi\rangle}&=\langle\Psi|H|\Psi\rangle_c\\&\cong\langle0|H|0\rangle-(\eta/2)\langle0|\{W,H\}|0\rangle_c\\&\quad+(\eta^2/8)\langle0|\{W,\{W,H\}\}|0\rangle_c\ .\end{aligned} \tag{4.13a}$$

Applying this with (4.12) on (4.6) gives

$$\begin{aligned}\langle\Psi|H|\Psi\rangle_c&\cong\langle0|J\mathcal{J}/2|0\rangle\\&\quad+(\eta^2/8)\langle0|\{W,\{W,J\mathcal{J}/2\}\}|0\rangle_c\\&\quad-(\eta/2)\langle0|\{W,I\mathcal{V}\}|0\rangle_c\ .\end{aligned} \tag{4.13b}$$

All diagrams up to second order are presented in Fig. 6. Nonzero contributions of first, second, and third terms of (4.13b) come from diagrams a, e, and h, respectively. Their contributions are written as

$$\begin{aligned}\langle\Psi|H|\Psi\rangle_c&=J\sum_{\sigma,j}[1-(-1)^j\delta_\sigma](P^\sigma_{j,j+1}+\tfrac{1}{8}\eta^2G^\sigma_{j,j+1})\\&\quad-\eta I\sum_{i,j}(P^\sigma_{i,j}P^{\bar\sigma}_{i,j})^2\ ,\end{aligned} \tag{4.14}$$

where

$$\begin{aligned}G^\sigma_{j,j+1}&=\tfrac{1}{2}P^\sigma_{j,j+1}+2P^\sigma_{j,j+1}P^{\bar\sigma\,2}_{j,j+1}\\&\quad-8\sum_{mn}P^{\bar\sigma\,2}_{m,n}P^\sigma_{m,n}P^\sigma_{n,j}P^\sigma_{m,j+1}\end{aligned}$$

and

$$P^\sigma_{ij}=\langle0|a^\dagger_{i,\sigma}a_{j,\sigma}|0\rangle\ .$$

Here, $\bar\sigma$ takes the opposite value of $\sigma=(u,d)$. In case of a uniform ladder ($\delta_\sigma=\Gamma_\sigma=0$) we can compute (4.14) exactly. In this case, after minimization one obtains

$$\varepsilon=E/2N=-J[1+\zeta(I/2J)^2]\ , \tag{4.15}$$

where $\zeta=0.0621$. Horsh[36] presented $\zeta=0.0680$, the difference coming from the fact that $|\Psi\rangle$ is not actually the real wave function of the system. This difference is not important if $|I|$ is small as it is needed to keep (4.13)

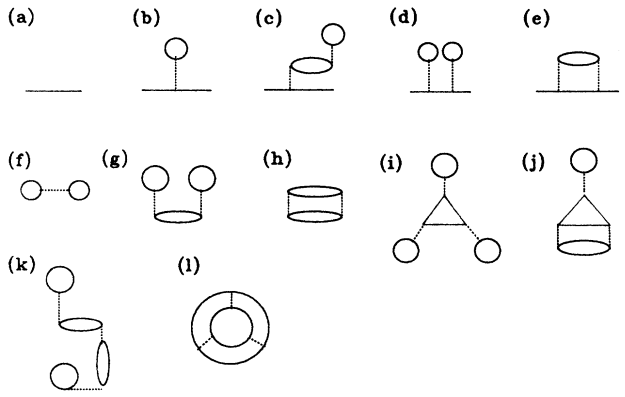

FIG. 6. Diagrams (a) to (e) and diagrams (f) to (l) are, respectively, the intrachain and the interchain contributions diagrams up to second order of Eq. (4.13a). In diagrams (a) to (e), all interaction lines (dotted lines) have η strength where for diagrams (f) to (l) one dotted line has I strength and the remaining have η. Nonnull contributions come only from diagrams (a), (e), and (h). A way to verify this is to note that η appears in Eq. (4.13b) with an even power in the kinetic part (J) and with an odd power in the interacting part (I). This means that diagrams (b), (f), (i), (j), (k), and (l) must be zero. As a consequence of being partly built with (b), diagrams (c), (d), and (g) will also have a null contribution.

valid.

In the dimerized state, the sum in (4.14) is computed up to third neighbors and the energy functional ε up to order δ^2, Γ^2, and $\delta\Gamma$ is obtained:

$$\varepsilon=\frac{J}{2}\left[\frac{2}{\pi}a_0 A\eta^2-b_0\frac{BI\eta}{2J}+C\right], \tag{4.16}$$

where

$$A=1+\frac{1}{a_0}[a_1\Gamma^2(\Lambda-1)^2-a_2\Gamma^2(\Lambda-\tfrac{3}{2})+a_3\Gamma\delta(\Lambda-1)],$$

$$B=1+(1/b_0)[b_1\Gamma^2(\Lambda-1)^2-b_2\Gamma^2(\Lambda-\tfrac{3}{2})],$$

$$C=\frac{2\delta^2}{\pi\lambda}-\frac{4}{\pi}\left[1-\frac{\Gamma^2}{2}(\Lambda-\tfrac{3}{2})+\Gamma\delta(\Lambda-1)\right],$$

and $\delta=|\delta_\sigma|$. For a "P" dimerization the a_i and b_i ($i=1,2,3$), are given by

$$a_0=\tfrac{1}{8}+6/\pi^4,\quad a_1=28/\pi^4,$$

$$a_2=\tfrac{1}{16}+15/\pi^4,\quad a_3=\tfrac{1}{8}-2/\pi^4,$$

$$b_0=\tfrac{1}{4}+8/\pi^4,\quad b_1=48/\pi^4,\quad b_2=16/\pi^4.$$

For an "A" dimerization, only a_1, a_3, and b_1 need to be changed:

$$a_1=-12/\pi^4,\quad a_3=\tfrac{1}{8}+6/\pi^4,\quad b_1=-16/\pi^4.$$

Minimization of ε, (4.16), with respect of η, δ, and Γ gives

$$\eta=\frac{\hat{I}B}{A},\quad \hat{I}=\frac{Ic_0}{2J},\quad \delta=\Gamma(1-c_1\hat{I}^2)\lambda/2\tilde{\lambda},$$

$$\tilde{\lambda}=\left[\frac{\lambda}{2}(1-c_1\hat{I}^2)^2+c_2\hat{I}^2\right]/(1-2c_3\hat{I}^2),$$

$$\Gamma=4e^{-\Lambda},\quad \Lambda=1+1/2\tilde{\lambda}, \tag{4.17}$$

$$\frac{\varepsilon}{J}=\frac{E}{2NJ}=-\frac{1}{\pi}-\frac{I^2}{2\pi}a_0-\frac{1}{4\pi}(1-2c_3\hat{I}^2)\Gamma^2,$$

where

$$c_0=\frac{\pi}{4a_0}b_0,\quad c_1=a_3/2,$$

$$c_2=a_0b_1/b_0-a_1/2,\quad c_3=a_2/2-a_0b_2/b_0.$$

These expressions are very similar to those of Baeriswyl and Maki. The differences come from the following: the possibility in our case of two different types of dimerization, the replacement of λ by $\lambda/2$ in $\tilde{\lambda}$ results from the presence of two chains, the bandwidth $2t_0$ for the tight binding band is replaced by J and finally for the spin-number normalization factor. We verify in (4.17) that ε, δ, and Γ are even function of I and that η is an odd function of I. For $\delta=0$, $\Gamma=0$ we get from (4.17) the same expression than (4.15) but with $\zeta=0.0580$. It indicates the effect of neglecting neighbors farther than the third one in computing (4.14).

Figures 7, 8, and 9 show the $|I/2J|$ dependence of Γ, δ, and $\Delta\varepsilon=\varepsilon-\varepsilon_0$ for three spin-phonon coupling ($\lambda=0.2$, 0.4, and 0.6). $\Delta\varepsilon$ is the difference in energy between that of the dimerized state, ε, computed with (4.16) and that of the uniform state, ε_0, computed using (3.3a). All these results are presented for both types of dimerization: P (dotted curves) and A (full curves). P's data reproduce the behavior noted in Ref. 35 for the Hubbard model. However for the A type dimerization, δ and Γ decrease for increasing $|I/2J|$. From the energy curves it is clear that the P dimerization is preferred over the A dimerization for $0.0<|I/2J|<1.0$. For small spin-phonon coupling λ, the dimerized states are preferred over the uniform states for small value of $|I/2J|$. On the other hand we found that η, is only weakly affected by the spin-phonon coupling λ and by the type of dimerization. In conclusion, our results show that at $T=0$ K, for $|I/2J|\ll 1$ and relatively small spin-phonon coupling λ (<0.6), the XY-Ising ladder is in a dimerized P state. Now, we have to verify if this behavior persists at very large interchain coupling.

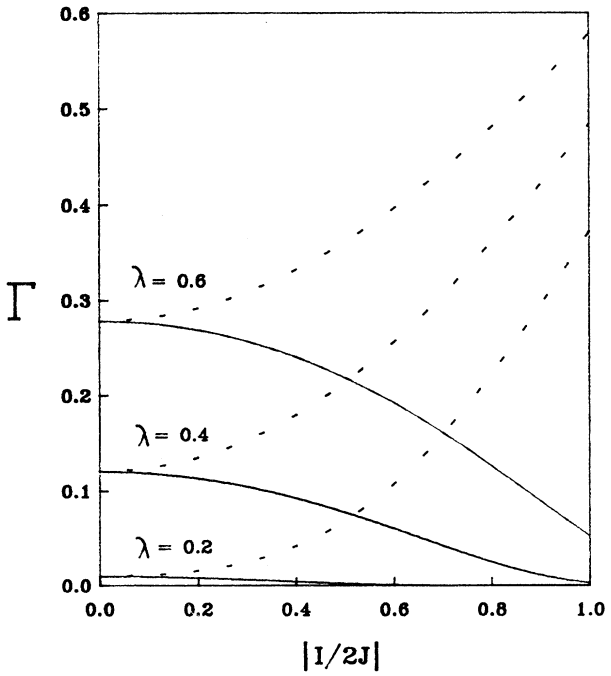

FIG. 7. Dimerization gap, Γ, as a function of $|I/2J|$ for some values of spin-phonon coupling $\lambda=0.2$, 0.4, and 0.6. Dotted curves are for "in phase" dimerization and continuous curves for "antiphase" dimerization.

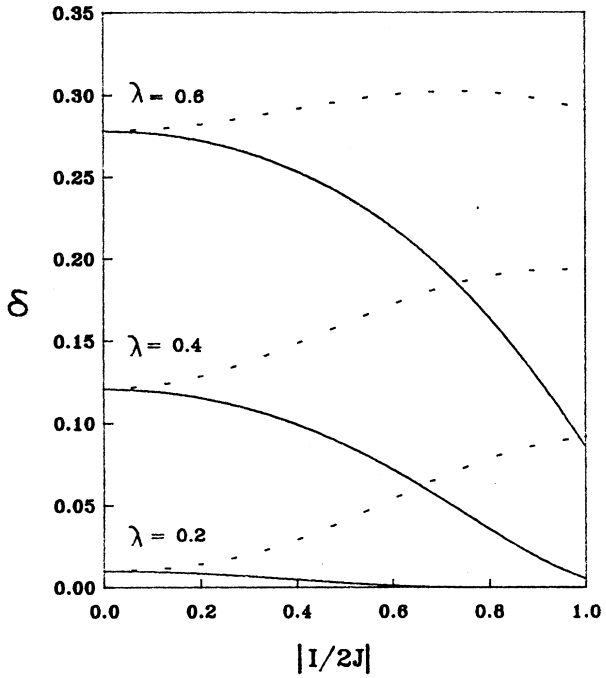

FIG. 8. Relative amplitude of dimerization, δ, as a function of $|I/2J|$ for some values of spin-phonon coupling $\lambda=0.2$, 0.4, and 0.6. Dotted curves are for "in phase" dimerization and continuous curves for "antiphase" dimerization.

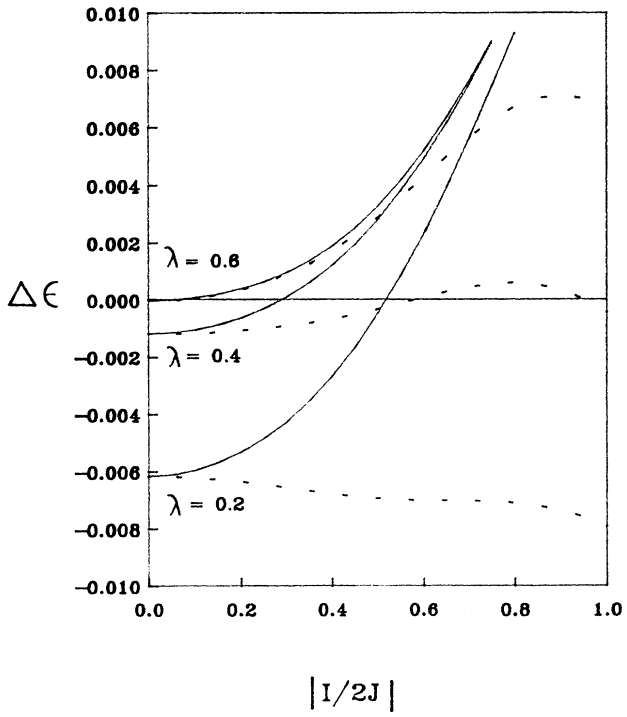

FIG. 9. Energy difference $\Delta\varepsilon=\varepsilon-\varepsilon_0$ between the variational result for finite dimerization amplitude and the exact result for the uniform bond case. Dotted curves are for "in phase" dimerization and continuous curves for "antiphase" dimerization.

B. Large interchain coupling

For $|I/2J|\gg 1$ we use second-order perturbation theory. The Hamiltonian is rewritten using H_1 and H_2:

$$H_1=I\sum_{\sigma,j}(n_{j,\sigma}-\tfrac{1}{2})(n_{j,\sigma}-\tfrac{1}{2}) ,$$
$$H_2=\tfrac{1}{2}\sum_{\sigma,j}J_{j,\sigma}(a^{\dagger}_{j,\sigma}a_{j+1,\sigma}+\text{H.c.}) . \tag{4.18}$$

The perturbation term is H_2. Its effect is computed by taking the fundamental of H_1 for half-filled band and the first excited state that can be reached via H_2. The energy of this excited state is $|I|$ above the fundamental. Using the same idea as Emery[37] and Cleveland and Medina,[38] for the dimerized system P or A, taking care of our σ dependence in $J_{j,\sigma}$ [see (4.3)], and using the following definition:

$$T^z_j=(n_{j,u}-n_{j,d})/2,\quad T^+_j=a^{\dagger}_{j,u}a_{j,d},\quad T^-_j=a^{\dagger}_{j,d}a_{j,u} ,$$

for $I>0$ and

$$T^z_j=(n_{j,u}+n_{j,d}-1)/2,\quad T^+_j=a^{\dagger}_{j,u}a^{\dagger}_{j,d}e^{i\pi j} ,$$
$$T^-_j=a_{j,d}a_{j,u}e^{-i\pi j} ,$$

for $I<0$, we obtain

$$H^P_{\text{eff}}=2J_{\text{eff}}\sum_j[1-(-1)^j\tilde{\delta}]\mathbf{T}_j\cdot\mathbf{T}_{j+1}+H' \tag{4.19}$$

and

$$H^A_{\text{eff}}=2J_{\text{eff}}\sum_j\{T^z_jT^z_{j+1}+(1-\alpha)(T^x_jT^x_{j+1}+T^y_jT^y_{j+1})\}$$
$$+H' , \tag{4.20}$$

where

$$H'=\frac{NJ}{4\pi\tilde{\lambda}}\delta^2-\frac{NJ^2}{4|I|}-\frac{N|I|}{4} ,$$
$$\tilde{\lambda}=\lambda/(2-\pi J\lambda/|I|) ,$$
$$J_{\text{eff}}=J^2(1+\delta^2)/2|I| , \tag{4.21}$$
$$\tilde{\delta}=2\delta/(1+\delta^2),\quad 1-\alpha=(1-\delta^2)/(1+\delta^2) ,$$

and λ is the spin-phonon coupling constant which has here the same definition as in Eq. (4.10). The component of vector operators $\mathbf{T}_j$ verify the spin-half commutation rules. H^P_{eff} is like the Hamiltonian of a dimerized Heisenberg chain. H^A_{eff} is like an Heisenberg anisotropic Hamiltonian where α is the anisotropy. The contribution of an applied magnetic field on the original spin ladder [$\gamma=0$ in Eq. (2.1)] is written here as $-h\sum_j T^z_j$ for $I<0$ and is 0 for $I>0$. Then in the strong coupling limit and small h ($h\ll|I|$), the magnetic susceptibility of the dimerized spin ladder will show, for $I<0$, exactly the same behavior as the dimerized or as the anisotropic Heisenberg chain depending on the type of dimerization (P or A) of the spin ladder. For $I>0$ it will give a very small response. It is worthwhile to note that a very small susceptibility is also expected at low temperature in the strong interchain coupling limit of the XY-XY ladder and the antiferromagnetic Heisenberg-Heisenberg ladder, since there is an en-

ergy gap proportional to this coupling between the fundamental and the first magnetic exited state of each quasi-independent rung.

In Fig. 10 curves of $E_{P(A)}=(\langle H_{\rm eff}^{P(A)}\rangle-\langle H'\rangle)/2N$ are given as functions of δ. E_P is calculated from Cross and Fisher relation:[39]

$$E_P\cong\frac{J^2}{4|I|}(1+\delta^2)(E_0-A\tilde{\delta}^{4/3}),$$

where $E_0=-0.886$ and $A=0.614$ is fixed by the numerical work of Bonner and Blöte.[40] To get E_A we used Orbach's numerical data, $E_{\rm Orb}$:[41]

$$E_A=-\frac{J^2}{4|I|}(1+\delta^2)E_{\rm Orb}(\delta)$$

with $\delta=\sqrt{\alpha/(2-\alpha)}$.

From Fig. 10 it is very clear that, excluding the free phonon part, the P dimerization has the lowest energy than the A dimerization or the uniform state ($\delta=0$). Then, the P dimerization is preferred to the A one for all dimerization amplitude. Coming back to the Cross and Fisher relation, the energy and the energy gap become

$$E\cong\frac{J_{\rm eff}}{2}(E_0-A\tilde{\delta}^{4/3})+\frac{J}{8\pi\tilde{\lambda}}\tilde{\delta}^2-\frac{J^2}{8|I|}, \tag{4.22}$$

$$\Delta=J\Gamma\sim J_{\rm eff}^{1/3}(J_{\rm eff}\tilde{\delta})^{2/3}. \tag{4.23}$$

Minimizing E and neglecting terms smaller than $\delta^2(\delta^2\ll1)$ we get the $|I/2J|$ dependence of the dimerization amplitude and gap:

$$\delta=4(2/3)^{3/2}\left[\frac{A}{E_0+|I|/2\pi\tilde{\lambda}J}\right]^{3/2}$$
$$\approx|2\pi\tilde{\lambda}J/I|^{3/2}. \tag{4.24}$$

And $\Gamma\propto(J/I)^2$. The same dependence was found for Γ by others[42,43] in the Hubbard model case with $I/2J\gg0$.

V. CONCLUSION: THE FUNDAMENTAL STATE AT $T=0$ K

We have shown that the XY-Ising ladder with a small mean-field spin-phonon interaction is, at $T=0$ K, in a dimerized state in which the dimers of the two chains are in front of each others, i.e., the dimerization in phase (P) state. We propose the conjecture that this state persists for all finite value of $|I/2J|$. The I dependence of the dimerization gap, Fig. 11, gives a summary of our results. This result, as long as only the P dimerization is concerned and in spite of the possibility of an A dimerization, is the same qualitative behavior predicted for the Hubbard model.[44–48] It is an even function of I, increasing with $|I|$ for $|I/2J|\ll1$, decreasing for $|I/2J|\gg1$ with a maximum expected between these two regimes.

Our explanation of the $|I|$ dependence of Γ in the ladder mode can be seen as following. For $I=0$, the spin chains are two independent systems. For $I\neq0$ and small, correlations are produced between a pair of spins of the same ladder rung (parallel spins for $I<0$ and antiparallel spins for $I>0$). Single-spin exchange through $J_{j,\sigma}$ breaks these correlations which can be restored, however, by the correlated exchange of the companion spin of the other chain. As a consequence, the two system of spins are

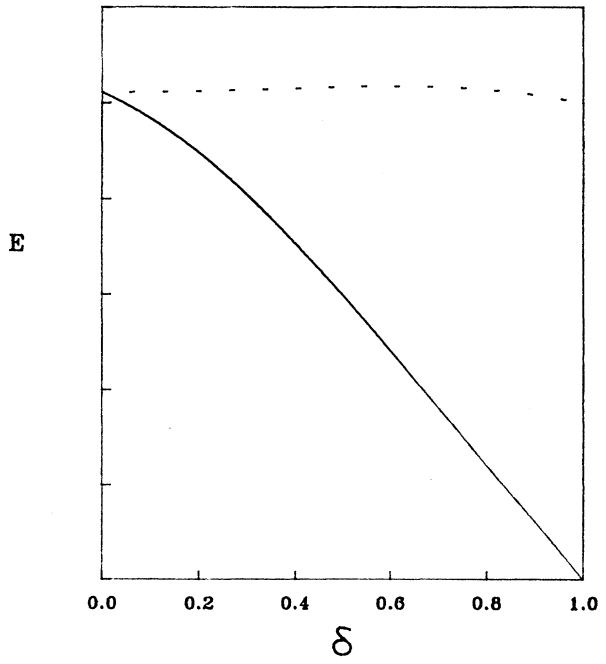

FIG. 10. Energy as a function of dimerization amplitude δ in the strong interchain coupling limit. The dotted curve is for the "antiphase" and the full curve is for "in phase" dimerization.

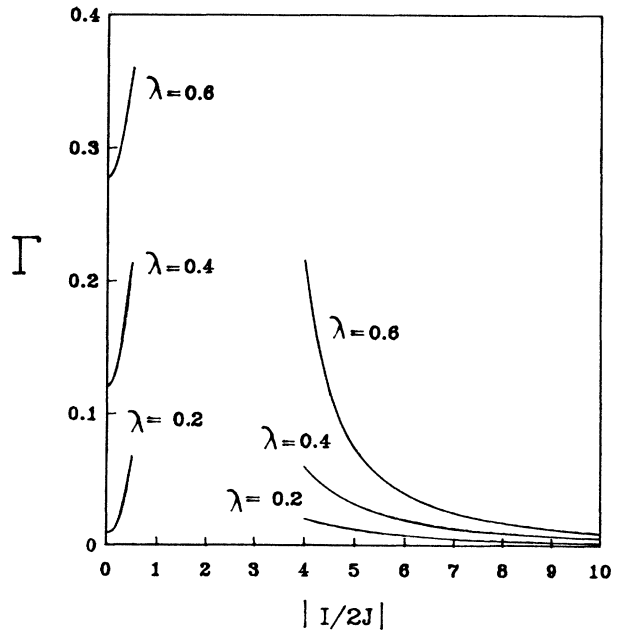

FIG. 11. Our results for the dimerization gap as a function of $|I/2J|$ in the small and large interchain coupling limit.

now synchronized and the response function N_{TP} is enhanced above N_{TA} since each spin in a correlated pair tries to follow the other. In the strong coupling limit, however, the response function N_{TP} decreases since the pairs of spins are correlated (localized) on sites and the exchange motion is frozen out.

In this study we neglected quantum fluctuations of phonons. These may be very important if the energy of free phonons is of the same order than the dimerization gap, $J\Gamma$. As a result, the quantum fluctuations of phonon fluctuations, together with large $|I/2J|$ and $\langle S^z \rangle$ fluctuations, may destroy the dimerized state. Impurities contributions can also be invoked to explain the great number of low-dimensional magnetic compounds that do not show the expected spin-Peierls transition.

ACKNOWLEDGMENTS

We thank Dr. Pravbov Shukla, Dr. Laurent, G. Caron, and Dr. Claude Bourbonnais for useful discussions. This work was supported by the Natural Sciences and Engineering Research Council of Canada, by the Fonds pour la formation de chercheurs et l'aide à la recherche du Québec and by the Centre de Recherche en Physique du Solide de l'Université de Sherbrooke.

[1]J. W. Bray, H. R. Hart, Jr., L. V. Interrante, I. S. Jacobs, J. S. Kasper, G. D. Watkin, S. H. Wee, and J. C. Bonner, Phys. Rev. Lett. **35**, 744 (1975).
[2]J. W. Bray, L. V. Interrante, I. S. Jacobs, and J. C. Bonner, in *Extended Linear Chain Compounds,* edited by J. S. Miller (Plenum, New York, 1982), and references therein.
[3]K. M. Diederix, H. W. J. Blöte, J. P. Groen, T. O. Klassen, and N. J. Poulis, Phys. Rev. B **19**, 420 (1979).
[4]D. Block, J. Voiron, and L. J. de Jongh, in *High Field Magnetism,* edited by M. Date (North-Holland, Amsterdam, 1893).
[5]R. A. T. Lima and C. Tsallis, Phys. Rev. B **27**, 6896 (1983).
[6]Y. Lépine, C. Tannous, and A. Caillé, Phys. Rev. B **20**, 3753 (1979); C. Tannous and A. Caillé, Can. J. Phys. **57**, 508 (1979). E. Pytte, Phys. Rev. B **10**, 4637 (1974).
[7]A. Kotani and I. Harada, J. Phys. Soc. Jpn. **49**, 535 (1980).
[8]Y. Lépine and A. Caillé, J. Chem. Phys. **67**, 5598 (1977).
[9]P. D. Loly, Y. Lépine, and A. Caillé, J. Phys. C **18**, 3779 (1985).
[10]J. Y. Dubois and J. P. Carton, J. Phys. (Paris) **35**, 371 (1979).
[11]R. A. T. Lima and C. Tsallis, Solid State Commun. **40**, 155 (1981).
[12]G. Beni and P. Pincus, J. Chem. Phys. **57**, 3531 (1972).
[13]J. C. Bonner and M. E. Fisher, Phys. Rev. **135**, A640 (1964).
[14]B. R. Patyal, B. L. Scott, and R. D. Willett, Phys. Rev. B **15**, 1657 (1990).
[15]D. C. Johnston, J. W. Johnson, D. P. Goshorn, and A. J. Jacobson, Phys. Rev. B **35**, 219 (1987).
[16]W. E. Hatfield, J. Appl. Phys. **52**, 1985 (1981); W. E. March, J. H. Helms, and W. E. Hatfield, Inorg. Chem. Acta **150**, 35 (1988).
[17]E. Dagotto and A. Moreo, Phys. Rev. B **39**, 5087 (1990).
[18]D. B. Brown, J. A. Donner, J. W. Hall, S. R. Wilson, S. B. Wilson, D. J. Hodgson, and W. E. Hatfield, Inorg. Chem. **18**, 2635 (1979).
[19]A. de Kozak, M. Samouël, M. Leblanc, G. Ferey, and J. Pannetier, Solid State Commun. **55**, 887 (1985); M. Vlasse, J. P. Chaminade, J. M. Dance, M. Saux, and P. Hazenmuller, J. Solid State Chem. **41**, 272 (1982).
[20]D. Babel and G. Z. Knobe, Anorg. Allg. Chem. **442**, 333 (1978).
[21]R. L. Carlin, J. Appl. Phys. **52**, 1993 (1981).
[22]J. V. Emery, in *Highly Conducting One Dimensional Solids,* edited by J. T. Devreese, R. P. Evrard, and V. E. van Doren (Plenum, New York, 1979) p. 274.
[23]E. H. Lieb and F. Y. Wu, Phys. Rev. Lett. **20**, 1445 (1968).
[24]H. Shiba, Phys. Rev. B **6**, 930 (1972).
[25]R. P. Feynman, Phys. Rev. **56**, 340 (1939).
[26]A. A. Ovchinnikov, Zh. Eksp. Teor. Fiz. **57**, 2137 (1969) [Sov. Phys. JETP **30**, 1160 (1970)].
[27]F. Woynarovich, J. Phys. C **16**, 6593 (1983).
[28]H. Shiba and P. Pincus, Phys. Rev. B **5**, 1966 (1972).
[29]H. Shiba, H. Progr. Theor. Phys. **48**, 2171 (1972).
[30]K. Subbarao and V. A. Singh, Phys. Rev. B **26**, 3788 (1982).
[31]S. Doniach, *Green's Functions For Solid State Physicist* (Benjamin, Ontario, 1974).
[32]T. Izuyama, D. J. Kim, and R. Kubo, J. Phys. Soc. Jpn. **18**, 1025 (1963).
[33]J. Hubbard and K. P. Jain, J. Phys. C **1**, 1650 (1968).
[34]M. Takahashi, Progr. Theor. Phys. **42**, 1098 (1969); **43**, 860 (1970); **43**, 1619 (1970).
[35]D. Baeriswyl and K. Maki, Phys. Rev. B **31**, 6633 (1985).
[36]P. Horsch, Phys. Rev. B **24**, 7351 (1981).
[37]V. J. Emery, Phys. Rev. B **14**, 2989 (1976).
[38]C. L. Cleveland and R. Medina, Am. J. Phys. **44**, 44 (1976).
[39]M. C. Cross and D. S. Fischer, Phys. Rev. B **19**, 402 (1979).
[40]J. C. Bonner and H. W. J. Blöte, Phys. Rev. B **25**, 6959 (1982).
[41]R. Orbach, Phys. Rev. **112**, 309 (1958).
[42]J. E. Hirsh and D. J. Scalapino, Phys. Rev. B **29**, 5554 (1984).
[43]H. J. Schulz, in *Low-Dimensional Conductors and Semiconductors,* edited by D. Jérome and L. G. Caron (Plenum, New York, 1986), p. 95.
[44]J. E. Hirsh, Phys. Rev. Lett. **51**, 296 (1983).
[45]S. N. Dixit and S. Mazumkar, Phys. Rev. B **29**, 1824 (1984).
[46]L. G. Caron and C. Bourbonnais, Phys. Rev. B **29**, 4230 (1984).
[47]G. W. Hayden and E. J. Mele, Phys. Rev. B **32**, 6527 (1985).
[48]L. Hubert, Phys. Rev. B **36**, 6175 (1987).